

SEISMIC RESPONSES OF CIVIL ENGINEERING STRUCTURES USING SOIL-STRUCTURE INTERACTION SYSTEM CONSIDERING NONLINEARITY OF REINFORCED CONCRETE AND SOIL

Yoshihiro Shishikura¹, Wataru Hotta², and Kazuaki Watanabe³

¹ Engineer, Taisei Corporation, Tokyo, Japan (sskysh00@pub.taisei.co.jp)

² Manager, Taisei Corporation, Tokyo, Japan

³ Acting General Manager, Taisei Corporation, Tokyo, Japan

ABSTRACT

Accurate analysis of soil–structure interactions is essential for assessing the seismic performance of underground structures. This study analyzes how the interaction between soil and structures in an intake pit with complex interference between structures (such as screen section and pumping room) affects the dynamic responses. The analysis was conducted using a three-dimensional finite element method (FEM) model that incorporated a soil–structure interaction (SSI) system. Seismic analysis accounts for the nonlinearity by considering liquefaction, reinforced concrete, and the contact surface between the soil and structures. The results show that three-dimensional seismic analysis provides more rational responses to seismic assessment than those determined using two-dimensional methods.

INTRODUCTION

Seismic assessments of underground structures, such as box culverts, have mainly focused on two-dimensional (2D) dynamic analyses in the transverse direction. However, in the cases of underground structures with complex three-dimensional (3D) configurations, such as intake pits, which include features such as screen section and pumping room, the accurate evaluation of the three-dimensional seismic behavior using traditional 2D analysis methods has been challenging. Therefore, in recent years, attempts have been made to assess the overall seismic performance of underground structures by applying static loads to 3D models of these structures.

In this study, we aimed to verify the applicability of a three-dimensional dynamic analysis considering the soil–structure interaction (SSI) of an intake pit with complex structures. We constructed a model with >600000 degrees of freedom considering the nonlinearity of the ground, including liquefaction phenomena, the nonlinearity of the concrete based on crack formation considerations, and contact detachment among the soil and structures.

First, we compared a 2D analysis with equivalent stiffness in the depth direction and a 3D analysis to evaluate the seismic earth pressures affecting the structure. We then analyzed the differences in SSI between these two approaches. In addition, we analyzed the strain distribution of the structure model and the scalability of the execution time for the 3D analysis results to confirm their applicability to practical design.

MODEL CONSTRUCTION AND ANALYSIS CONDITIONS

The 3D analysis model is shown in Figures 1 and 2. The 2D analysis model is shown in Figure 3. The material properties are listed in Tables 1 and 2. The input seismic motions are shown in Figure 4.

The 3D analysis model employed a full-scale model containing >600000 degrees of freedom, representing both the soil and an intake pit (Figures 1 and 2). Specifically, the intake pit was intricately modeled considering complex structures, and the reinforcement was represented using embedded elements (Feenstra 1993). The nonlinearity of the soil constitutive behavior was captured using a model capable of reproducing liquefaction phenomena under effective stress conditions using the multiple

shear mechanism model (Iai 1992, Hotta 2019). The intake pit was modeled using the model proposed by Maekawa (Maekawa 2003, Yamashita 2011) that accurately represents the compressive, tensile, and shear behaviors of concrete. Conversely, the reinforcing bars were modeled using linear elements. The contact detachments between the soil and structures were represented using joint elements (Goodman 1968). Three-dimensional, dynamic finite element method (FEM) analyses based on the SSI system were conducted in the past. However, few studies have considered liquefaction, concrete cracking, and contact detachment simultaneously, as in this study. Analysis of the 3D model was performed using E-FrontISTR (Motoyama 2021), which is an extension of the open-source parallel FEM program FrontISTR (Github). The analysis was performed on a server equipped with the Intel central processing unit (CPU) for parallel computing. The Intel CPU used in this study has a fairly standard performance level in the high-performance computing field.

The 2D model also incorporated a representation of the soil and an intake pit (Figure 3). The same nonlinear constitutive rules were applied to both soil and joint elements. However, for the structure, an equivalent stiffness (linear) was obtained by averaging the rigidity of the intake pit. The analysis code for the 2D model utilized FLIP (FLIP Consortium).

The material properties and input seismic motion were set based on the JSEC 2021. The material properties are listed in Tables 1 and 2. The input seismic motions are shown in Figure 4. The input seismic motions were estimated from the 2004 Rumoi Earthquake waveform obtained from HKD020 (K-NET) of the NIED using 1D equivalent linearized method with reference to the CRIEPI report (Sato 2013), and the amplitudes were tuned. The analysis model was input simultaneously in the horizontal and vertical directions of the intake pit. The model was calculated for 20 s with a time step of 0.002 s; this resulted in 10000 steps. The lateral boundary conditions were set as free considering the sufficient size of the analysis region. In addition, a viscous boundary was established at the bottom part of the model.

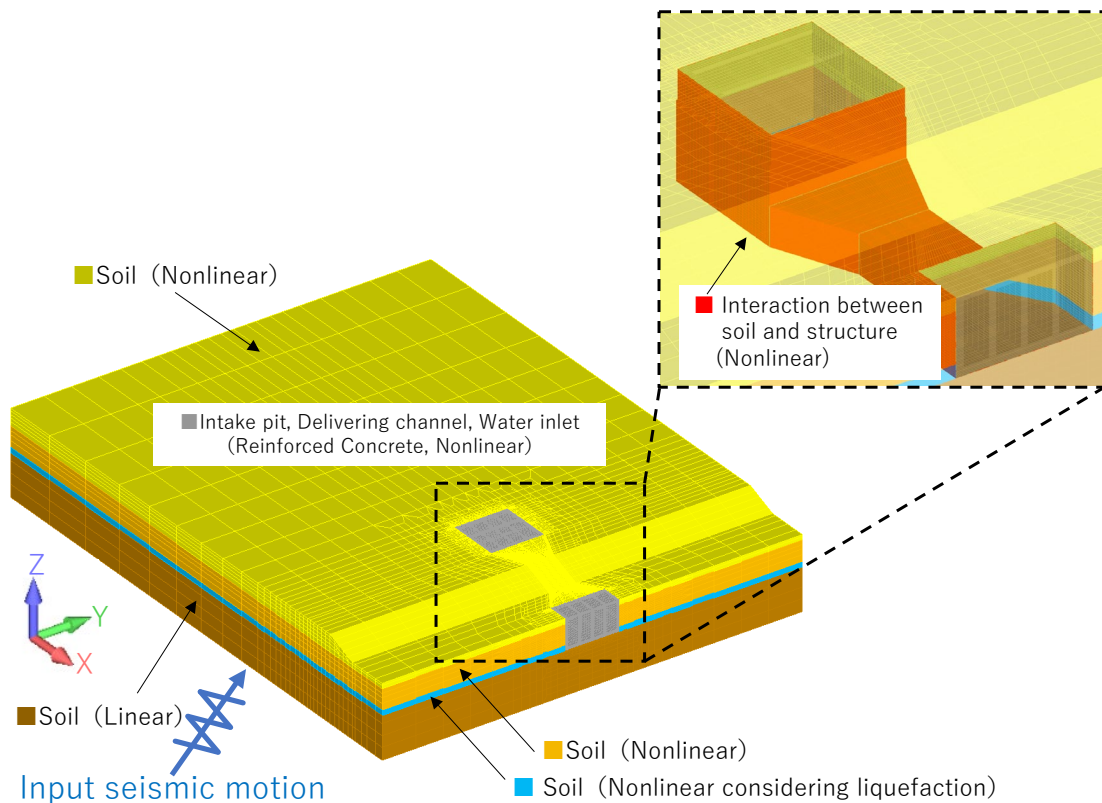


Figure 1. Seismic response analysis model (three-dimensional (3D) model)

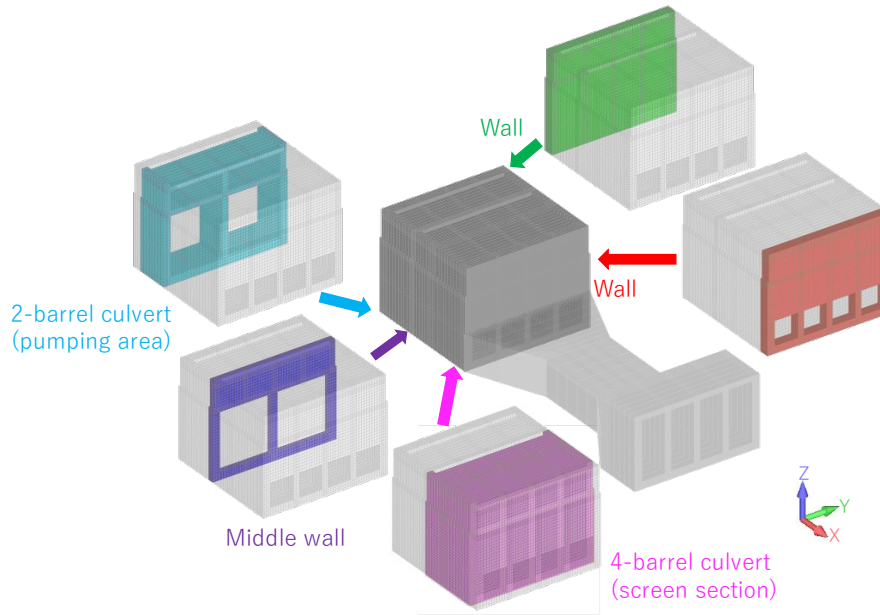


Figure 2. Intake pit (3D model)

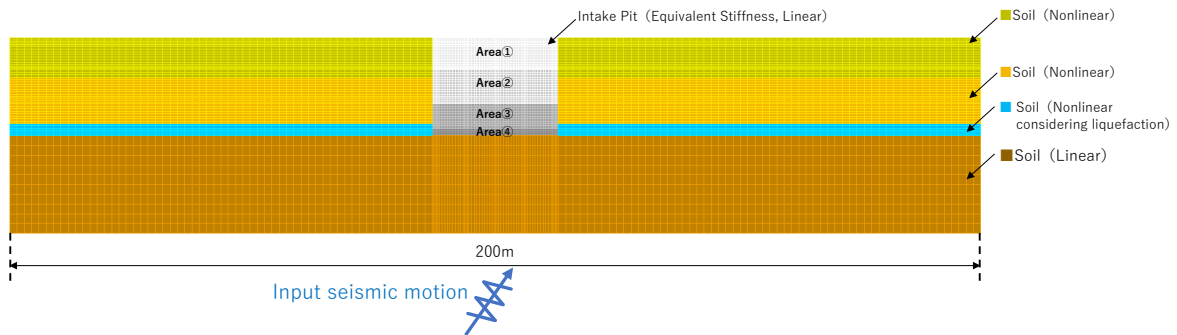


Figure 3. Seismic response analysis model (two-dimensional model)

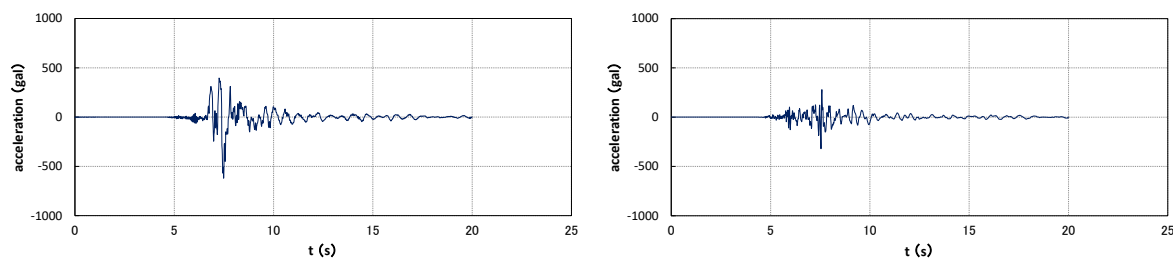
Table 1: Soil parameters

| | Type | Elevation [m] | Unit Weight ρ [t/m ³] | Poisson's Ratio ν | Initial Shear Modulus G_0 [kN/m ²] |
|---|------|---------------|--|-----------------------|--|
| Soil (Nonlinear) | Sand | 0.0 – +8.0 | 1.835 | 0.33 | 165000 |
| Soil (Nonlinear) | | -9.5 – 0.0 | 2.039 | 0.33 | 184000 |
| Soil (Nonlinear considering liquefaction) | | -12.0 – -9.5 | 2.039 | 0.33 | 184000 |
| Soil (Linear) | Rock | -32.0 – -12.0 | 2.039 | 0.33 | 990000 |

Table 2: Structural parameters

| | Unit Weight ρ [t/m ³] | Poisson's Ratio ν | Initial Shear Modulus G_0 [kN/m ²] |
|-------------------------|--|-----------------------|--|
| Three-dimensional model | 2.400 | 0.2 | 2300000 |

The two-dimensional model utilizes equivalent stiffness.



a) Horizontal seismic motion (Y-direction)

b) Vertical seismic motion (Z-direction)

Figure 4. Input seismic motions

COMPARISON FROM THE PERSPECTIVE OF SSI

In this section, we compare the earthquake-induced earth pressure acting on the structure using 3D and 2D analyses and analyze it from the perspective of SSI. Figures 5 and 6 show the displacement norm contours of the intake pit and the depth distribution of the stress in the ground elements adjacent to the structure when a horizontal deformation difference between the top and bottom occurs.

As shown in Figures 5 and 6, the 3D model reveals that the soil stress varies depending on the position of the member, thus confirming the occurrence of complex SSIs. Furthermore, in the 3D model, there was a noticeable trend of rapid stress changes within a narrow range near the overhang at the perimeter of the structure. This trend was not observed in the 2D model, which did not incorporate the overhang, thus confirming the effect of the structural shape on the SSI.

Figure 5 shows that the soil normal stress of the opening of the middle wall on the active side exhibits a significant decrease compared with that obtained when a 2D analysis is used. This was particularly evident for middle wall and 4-barrel culvert-1 located sufficiently far from the front and back walls. The normal soil stresses on the front and back walls tended to be higher than those in the 2D analysis. However, the distribution trend of the soil shear stress did not exhibit significant differences between the 3D and 2D analyses. This suggests a smaller influence of the complex shape of the structure and its nonlinearity compared with the normal stress of the soil. The stress distribution of the 2D model was distributed at the average position of the stress distribution of the 3D model, thus suggesting that it can adequately represent the average ground stresses acting on the structure.

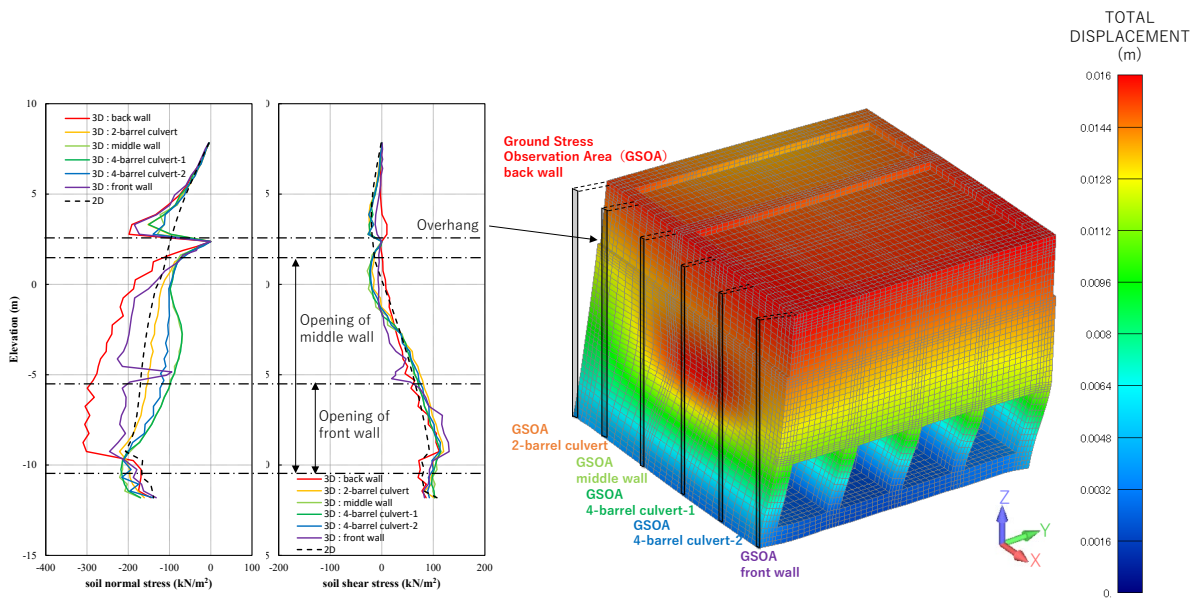
The deformation contours are shown in Figure 5. The locations where the normal stress of the soil decreased approximately coincided with the areas where the structure underwent extensive deformation. The increased deformation of the members resulted in a decrease in stiffness owing to plasticization, which led to a reduced displacement difference between the structure and the soil. Therefore, it could be inferred that at the opening of the middle wall, the reduction in the normal stress of the soil was caused by a decrease in the displacement difference between the structure and soil at the location where the deformation increased. Conversely, it is thought that for massive members such as the front and rear wall, which were less plasticized, the displacement difference with the soil increased, resulting in an increase in the normal stress. A localized decrease in the soil normal stress was observed at the corner openings of the front wall; this could be attributed to the occurrence of plasticization in these areas. It is worth noting that the plasticization status of the members will be discussed in subsequent sections, and it has been confirmed that there is a correspondence between the deformation of the structure and the plasticization status.

According to Figure 6, on the passive side, the normal stress of the back wall of the soil tended to decrease compared with that estimated using the 2D model. However, the normal soil stress at the opening of the front wall tended to exceed that of the 2D model. The stress distribution of the shear stress of the soil differed between the 3D model and the 2D model, with an increase in stress in the positive direction at the opening of the front wall and an increase in stress in the negative direction in

the massive area of the front wall. On the passive side, there were no distinct differences in stress distribution between the 3D and 2D models, as observed on the active side. The stress distribution of the other members did not exhibit noteworthy differences compared with those of the 2D model. This indicates that the 2D model adequately represents the average ground stress acting on the structure, even on the passive side.

The stress distribution trend on the passive side can also be examined by examining the displacement difference between the soil and structure. Specifically, it could be inferred that the decrease in displacement induced by the structure on the back wall side (where the structure has undergone minimal plastic deformation), leads to a reduction in the normal stress of the soil. In contrast, the increase in the normal stress on the soil in the front wall could be attributed to the increased displacement of the opening section, as observed from the deformation contours in Figure 6, thus indicating the influence of plasticization on the opening section. The increase in soil shear stress on the front wall can also be attributed to the decreased displacement difference between the structure and the soil.

Based on these results, it was confirmed that 3D analysis could evaluate the varying changes in the SSI for each member compared with 2D analysis conducted based on an equivalent stiffness. Therefore, to assess SSI precisely, it is crucial to model complex structures precisely using various features, such as shape, partitions, and openings, and to consider the nonlinearity of reinforced concrete. Moreover, because the SSI is dependent on the displacement difference between the ground and structure, it was shown that it is important to consider the nonlinear behavior of liquefiable ground as well as accurately model the contact detachment between the ground and structure.



a) Depth distribution of soil stress

b) Displacement contours (3D)

Figure 5. Depth distribution of soil stress (active side) and displacement contours

Figure 9 shows that the execution time for the 64 parallel cases in this study was approximately 30 h. Moreover, the analysis times for the 16, 32, and 192 parallel cases conducted as a parametric study yielded a linear relationship, thus confirming that the study model and analysis code, E-FrontISTR, had sufficient scalability. Based on these results, it is suggested that 3D dynamic nonlinear analysis with a detailed model of the structure and SSI could be applied in actual design practices by utilizing high-performance computing technology.

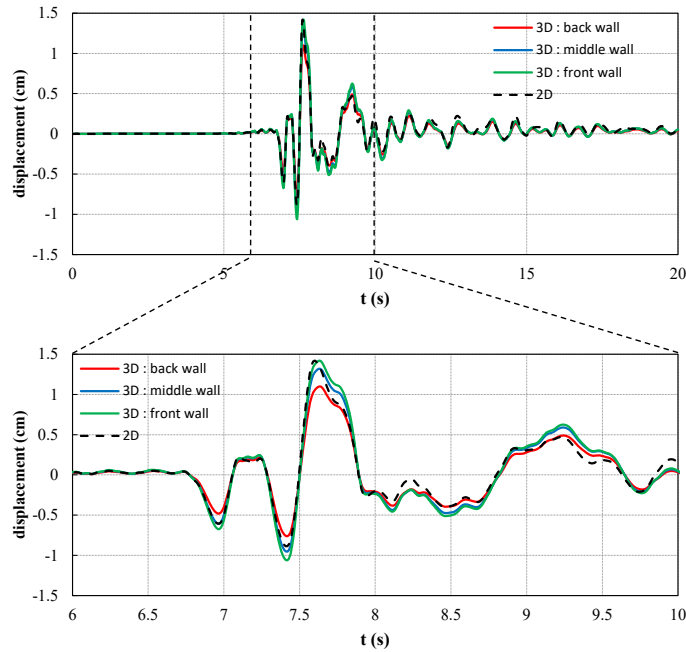


Figure 7. Time history of the horizontal deformation difference between the top and bottom parts of the structure

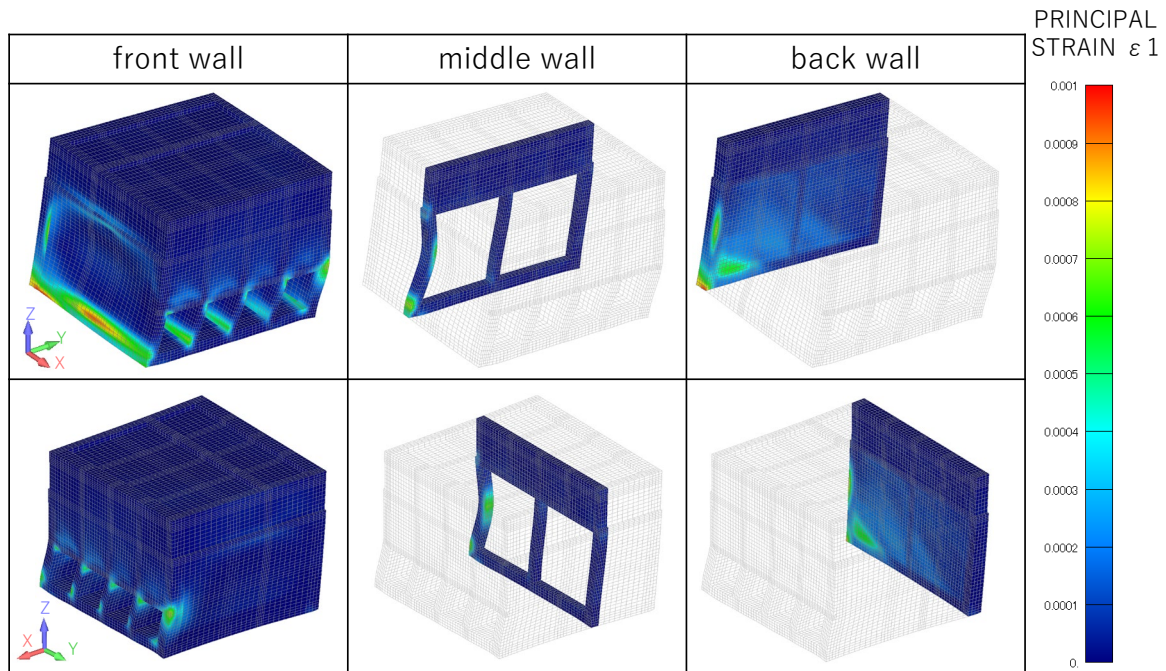


Figure 8. Maximum principal strain at the time at which the horizontal deformation difference between the top and bottom parts of the structure is maximized (section)

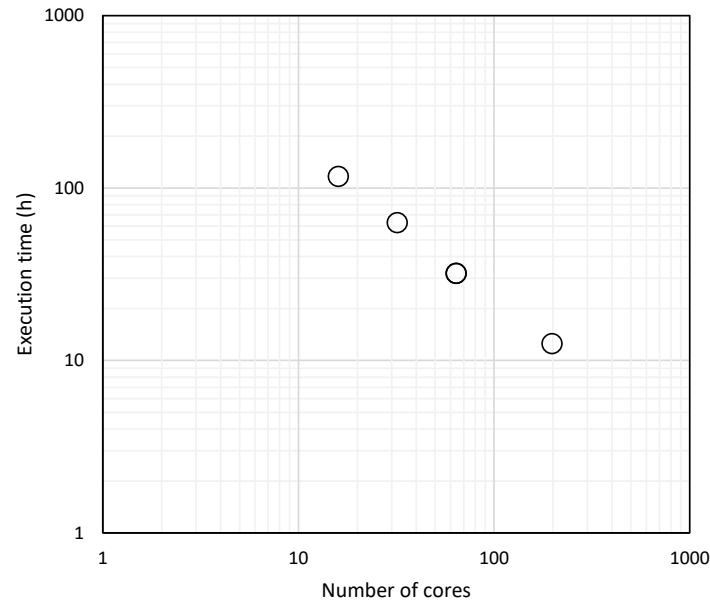


Figure 9. Scalability of computation

CONCLUSION

In this study, we confirmed the applicability of 3D dynamic analysis with SSI by modeling an intake pit and its surrounding soil (which featured complex structures) using a full-scale 3D FEM model comprising >600000 degrees of freedom. The analysis considered the nonlinearity of the ground, including liquefaction phenomena, nonlinearity of the concrete considering crack formation, and contact detachment between the soil and structures. The following conclusions were drawn.

The seismic earth pressures generated in the 3D model exhibited continuous variations in both the normal and shear stress directions along the depth direction of the intake pit, thus reflecting the differences in the cross-sectional shape and indicating the complex behavior of the SSI. Moreover, the seismic earth pressures from the 3D model considering nonlinearity showed a tendency to decrease the normal stress compared with the 2D model with equivalent stiffness. Thus, considering the nonlinearity of the SSI in the 3D dynamic analysis enables a more rational design in terms of seismic loads acting on the structure.

The highly detailed 3D dynamic analysis, which modeled complex structures, allowed for the analysis of the intricate nonlinear behavior of concrete at individual locations, such as the localized strain concentration and deformation suppression. This facilitated a more rational design.

The execution time for the 3D dynamic nonlinear analysis was approximately 30 h, with 64 parallel computing processes for an input seismic motion of 10000 steps, thus demonstrating sufficient scalability. Therefore, 3D dynamic, nonlinear analysis could be applied to designs using high-performance computing technology.

REFERENCES

- Feenstra P.H., Computational Aspects of Biaxial Stress in Plain and Reinforced Concrete, PhD Thesis, Delft University of Technology, 1993.
- Committee of Civil Engineering of Nuclear Power Facilities (JSCE): *Seismic Performance Verification Guidelines for Critical Underground Reinforced Concrete Structures in Nuclear Plants*, 2021.
- Iai S, Matsunaga Y, Kameoka T. Strain space plasticity model for cyclic mobility. *Soils Found.* 1992;32(2):1–15.
- Hotta W, Suzuki S, Hori M. On contraction of three-dimensional multiple shear mechanism model for evaluation of large scale liquefaction using high performance computing. *Geosciences.* 2019;9(1):38.
- Maekawa K, Okamura H, Pimanmas A. *Non-Linear Mechanics of Reinforced Concrete*. Taylor & Francis; 2003.
- Yamashita T, Hori M, Oguni K, Okazawa S, Maki T, Takahashi Y. Reformulation of non-linear constitutive relations of concrete for largescale finite element method analysis. *J Japan Soc Civil Eng.* 2011;67(1):145–154 (in Japanese).
- Goodman RE, Taylor RL, Brekke TL. A model for the mechanics of jointed rocks. *J Soil Mech Found Div.* 1968;94(3):637–659.
- Motoyama H, Sawada M, Hotta W, Haba K, Otsuka Y, Akiba H, Hori M. Development of a general-purpose parallel finite element method for analyzing earthquake engineering problems. *Earthquake Engng Struct Dyn.* 2021;1–19.
- FrontISTR. <https://github.com/FrontISTR/FrontISTR> (Accessed February 22, 2021).
- FLIP Consortium. https://www.flip.or.jp/en/flip_english.html (Accessed December 1, 2023).
- National Research Institute for Earth Science and Disaster Resilience Strong-motion Seismograph Networks (K-NET, KiK-net). <https://www.kyoshin.bosai.go.jp/> (Accessed August 29 , 2023).
- Sato H, Shiba Y, Higashi S, Kunugi T, Maeda T, Fujiwara H. Estimation of basement earthquake motion and site characteristics at HKD020 during the 2004 Rumoi earthquake based on geophysical exploration and laboratory tests. CRIEPI Civil Engineering Research Laboratory Report No. N13007. 2013 (in Japanese).